

Improving fault tracing detection applying 3D ant tracking seismic attribute

Adel Ali Ali Othman, Mohamed Abdel Aziz Mohamed, and
Mohamed Fathi Mohamed

Benefits of applying Ant tracking seismic attribute over the Ras El-Ush area in the Southern part of the Gulf of Suez, Egypt.

Abstract: Fault detection is one of most important steps in seismic interpretation either in exploration or in development phase. There are a variety of seismic attributes enhancing fault visualization and detection already used by interpreters. The ant-tracking attribute is available in petrel software. It emulates the behavior of ant colonies in nature and how they use pheromones to mark their paths in order to optimize the search for food. What we have done is working on ant -tracking attribute, which is a very powerful attribute in fault detection that can give us fault patches both automatically and manually. In this study the general workflow, to get an acceptable and clear result, showing exact trend and path of faults, have been provided requiring considerable amount of manipulation on related parameters, each of which have discussed separately. Automatic extraction of fault surfaces also used from ant-tracking attribute cube which not only shows very good match to those manually interpreted but also some minor faults which can't be detected easily by routine interpretation.

I. Introduction

Seismic attribute is any measure of seismic data that helps us better visualize or quantify features of interpretation interest. Seismic attributes fall into two broad categories, namely those that help us to quantify the morphological component of seismic data, and those that help us to quantify the reflectivity component of seismic data. The morphological attributes help us to extract information on reflector dip, azimuth, and terminations that can be related to faults, channels, fractures, diapers, and carbonate buildups. The reflectivity attributes lead to extract information on reflector amplitude, waveform, and variation with illumination angle, which can be related to the lithology, reservoir thickness, and the presence of hydrocarbons.

In the reconnaissance mode, 3D seismic attributes help us to identify structural features and depositional environments. In the reservoir characterization mode, 3D seismic attributes are calibrated against real and simulated well data to identify hydrocarbon accumulations.

salt dome, the faults shadow and complex structure have impacted Ras El-ush seismic data and has resulted in multitude of noise and artifacts. Some faults are masked while other anomalies are generated by the salt formation.

In this paper, we used ant tracking seismic attribute methodology that enhance subtle changes in amplitude, phase and sensitive to errors as well as enhancements in processing to minimize seismic artifacts and calibrate the attribute expression of geologic features that were unrecognized or overlooked previously.

One of the main goals of this paper is to apply future advances in 3D structural seismic interpretation workflow Figure-1. Currently, several commercial workstation software packages allow interpreters to define/generate their own attributes from seismic or attribute data volumes and/or from picked surfaces and horizon attribute extractions. This development allows all interpreters whose programming skills are not sufficient for filling out a spreadsheet of developing innovative workflows.

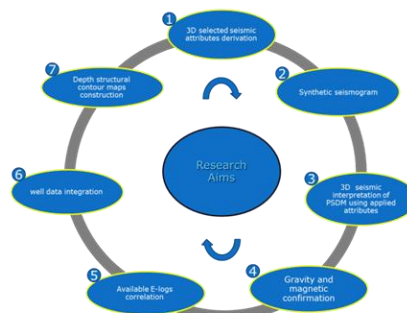


Figure-1: Schematic workflow shows the steps and procedures that have used for achieving the research aims.

II. Geological Framework

The Late Cenozoic Gulf of Suez Basin in Egypt is one of the best-studied examples of a continental rift. It is a failed intercontinental rift that forms the NW- SE trending continuation of the Red Sea rift system and has highly deformed Paleozoic-Cenozoic successions, with proven hydrocarbon reserves and excellent hydrocarbon potential with prospective sedimentary basin area measuring 19000 km². It is considered as a prolific oil province rift basin in Africa and Middle East (Al Sharhan, 2003). The opening of the Gulf of Suez was initiated during the Late Oligocene to Early Miocene by NE-SW separation of the African and Arabian plates. This opening was culminated with the Red Sea breakup in the Serravalian stage of the Miocene. The Gulf of Suez region was brought to its present configuration by the rift tectonics since latest Oligocene to Early Miocene (~25 Ma ago), which resulted in many tilted fault blocks of varying dimensions. These blocks were continuously active most of the Miocene time. The continuous rising and sinking contributed to great thickness and facies variations of the Miocene sediments. Several significant basins ward unconformities occur in the Gulf of Suez. These surfaces were primarily formed in response to regional tectonic adjustments associated with different phases of rift evolution (Dolson et al., 2001). The Gulf of Suez has been the focus of hydrocarbon exploration for over 100 years. The rift is up to 80 km wide and 300 km long, and comprises a series of classic half-graben tilted fault blocks, typically <20km wide and up to 50km long. The dip polarity of the fault blocks and their bounding faults change along the length of the rift, dividing the rift into three distinct large-scale half grabens. They alternate in polarity along the rift axis and are separated by major accommodation zones. One accommodation zone is located in the vicinity of the Morgan oil field and the second is situated east of the Galala Plateaux at Wadi Araba (Bosworth, 1985; Collette et al., 1988; Patton et al., 1994; Moustafa, 1996).

The stratigraphic setting and tectonic evolution of the Suez Gulf have been dealt by several authors: Said (1962), Beleity et al (1986), Barakat et al (1986), Moretti and Collette (1987), Meshref (1990), Tawfik et al (1992), Darwish and El-Araby (1993), Moustafa (1993 & 1996), Moustafa and El-Raey (1993), El-Barkooky and EL-Araby (1998), Bosworth and McClay (2001), Young et al (2003), El-Barkooky et al (2006), Leppard and Gawthorpe (2006), El-Azabi and EL-Araby (2007), El-Araby et al (2009) and others.

Major pre- and syn-rift source rocks have potential to yield oil and/or gas and are mature enough in the deep kitchens to generate hydrocarbons.

The pre-rift reservoirs in the Gulf of Suez include Precambrian fractured granite, Paleozoic- Lower Cretaceous sandstone (Sandstone of Nubian facies), Upper Cretaceous sandstone (i.e. Raha and Matulla Formations) and fractured Eocene Thebes Formation. The syn-rift reservoirs are represented by both sandstone and limestone facies belonging to Nukhul, Rudeis, Kareem and Belayim Formations.

Ras el Ush field, located in the southern part of the Gulf of Suez and is an offshore oil field located in the eastern side of Gabal El- Zeit (Figure-2), belongs to the southern sub province of the Gulf of Suez. All wells in this field are drilled directionally from land behind the coastline. They were drilled almost normal to the bedding of the strata at an average deviation angle of 60° to the northeast and east directions.

Ras El Ush Oil Field was discovered in February 1995. The production from this field started in early 1996, and presently producing from seven wells. These wells were drilled from shore with record deviation. The production comes from two pay zones, the Matulla sands with crude gravity of 34 API and Nubia sands with crude gravity 36 API. The daily production from the Field had peaked to 16,000 barrels in early 1998.

Ras El Ush Field in the centrally located Gebel El Zeit basement range, between East Zeit Trough, to the east and Gemsa Basin to the west. The granites basement complex of Gebel El Zeit represents the raised and eroded edge of a large rotated fault block. Southwest dipping Pre-Miocene, Miocene and younger sediments lie over the west side of the Gebel and become thicker into the large asymmetric Gemsa Basin. This is where the younger units fill successively underlying the sedimentary wedge.

The Western flank region of Gebel El Zeit is dissected by a series of easterly dipping, clysmic trending faults and NE-SW cross faults. Pre-Miocene sediments in the subsurface can read maximum dip rate of 35-40° to the South West in contrast to 15-20° South West dip observed in the shallower Miocene and younger units to the East.

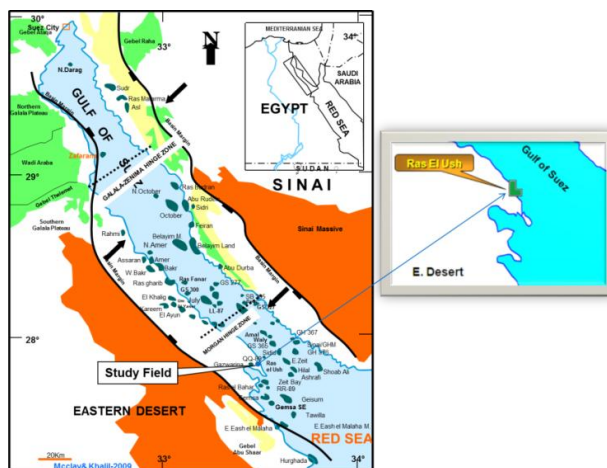


Figure 2: Structural map of the Gulf of Suez (Mcclay & Khalil-2009) associated with the location map of REU field, Egypt.

The interpretation of the major structural highs are based on the fault transfer model in which the cross fault link the individual segment of NW-SE high trend, along which proven Ras El Ush oil Field is located. These blocks seems to be offset-right stepping along the oblique faults. Untested structural high blocks were defined by this fault mechanism and were in good agreement with applied selected 3D seismic attributes. Ras El Ush trend would be high prospective and might reveal potential prospects (Mohamed Saleh et al 2009).

In Ras el Ush field, the main producing pay zones are represented by: Coniacian-Santonian Matulla Formation and Paleozoic-Lower Cretaceous Nubia Sandstone.

The stratigraphic section can be divided into three main tectonostratigraphic units: The pre-rift, syn-rift, and post rift units. Figure-3 Unit-I is represented by the pre-Miocene rocks that existed before the opening of the rift. These rocks include the Pre-Cambrian basement, Nubia Formation, Raha Formation in specific areas, Matulla Formation, Brown Limestone Formation, Sudr chalk Formation, Esna Shale Formation, and Thebes Formation. Unit-II is represented by the Miocene rocks deposited during the tectonic subsidence of the Suez rift in the study area; the syn-rift rocks include Basal Miocene Formation, Belayim Formation, South Gharip Formation, and Zeit Formation. Unit-III is represented by Pliocene Recent sediments which were deposited after the waning of tectonic subsidence of the rift.

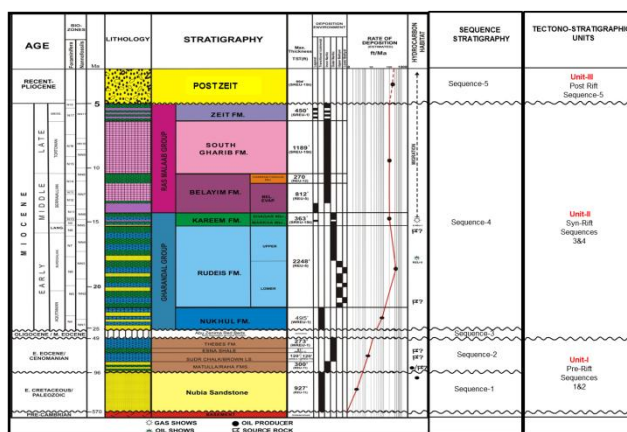


Figure-3: Generalized Stratigraphic Section and Hydrocarbon Habitat (Petrozeit 2011) of Ras El-Ush Field, Gulf of Suez, Egypt

III. Theory

Seismic attributes extract information from seismic reflection data that can be used for qualitative and quantitative interpretation. Attributes are used by geologists, geophysicists, and petrophysicists to map features from basin to reservoir scale. Some attributes, such as seismic amplitude, envelope, RMS amplitude, spectral magnitude, acoustic impedance, elastic impedance, and AVO are directly sensitive to changes in seismic impedance. Other attributes such as peak-to-trough thickness, peak frequency, and bandwidth are sensitive to layer thicknesses. Both classes of attributes can be quantitatively correlated to well control using multivariate

analysis, geostatistics, or neural networks. Seismic attributes such as coherence, Sobel filter-based edge detectors, amplitude gradients, dip-azimuth, curvature, and gray-level co-occurrence matrix measures are directly sensitive to seismic textures and morphology. Geologic models of deposition and structural deformation, coupled with seismic stratigraphy principles and seismic geomorphology, allow us to qualitatively predict geologic facies. In this paper, we present results from the most useful 3D seismic Ant tracking attribute analyses, dependent on the need of the geological features to enhance the detection of the clysmic fault-offsetting amount and the minor and major cross faults that passed through the study field.

IV. Ant tracking technique

Ant tracking attribute is an excellent technique for delineating geological boundaries (faults, stratigraphic contacts, etc.). It allows accelerated evaluation of large data sets. Also, it has the ability to provide quantitative estimate of fault/fracture presence and often enhances stratigraphic information that is otherwise difficult to extract.

This unique algorithm is part of an innovative workflow that introduces a new paradigm in fault interpretation. The procedure consists of four steps. The first step is to condition the seismic data by reducing noise in the data. The second step enhances the spatial discontinuities in the seismic data (fault attribute generation, edge detection). The third step, which generates the Ant track volume, significantly improves the fault attributes by suppressing noise and remains of non-faulting events. This is achieved by emulating the behavior of ant colonies in nature and how they use foramens to mark their paths in order to optimize the search for food. Similarly, "artificial ants" are put as seeds on a seismic discontinuity volume to look for fault zones. Virtual pheromones deployed by the ants capture information related to the fault zones in the volume. The result is an attribute volume that shows fault zones very sharp and detailed.

Ant Tracking is a CPU-intensive process. It is advisable to use a small-cropped volume first to test the parameters before attempting to calculate larger areas. As a rule of thumb, account for 20 min. of calculation for a 100-Megabyte volume using a machine with 2- Gigabyte of RAM and 1.7 GHz of CPU-clock. The time it takes to generate a volume will depend heavily on the amount of discontinuities that are present in the input volume and on the mode you are running the Ant tracking.

A coherent signal tracker is based on "swarm intelligence" to find optimal connectivity for fault features within an edge detected volume. The results are the basis for interpretation automation and allow the unique capability for orientation filtering.

As a first step in the Ant-track algorithm, each agent makes an initial estimate of orientation for the identified local maximum within the agent's territory (Ant boundary parameter). This orientation estimate will define the tracking direction for that agent. Within the program, the agents are restricted to a maximum of 15% deviation from this original orientation estimate. Also, the movement of the ant agents is performed in steps (Ant step size), a step being defined in voxels (Figure-4). Ant Boundaries are defined by a radius, in voxels for the distribution of the Ant agents. If the agent is unable to identify a local maximum or make an orientation estimate within this radius, the agent will be exterminated.

In the general, Ant tracking workflow, preprocessing (Figure-5) can involve preparing the seismic with structural smoothing, filtering or other attributes, followed by discontinuity attributes such as chaos (Randen et al., 2000) or variance (Van Bommel and Pepper, 2000). The resultant volume(s) are tracked by the "ant" agents, which are tuned to follow the desired faults while avoiding known noise sources (e.g. survey overprint).

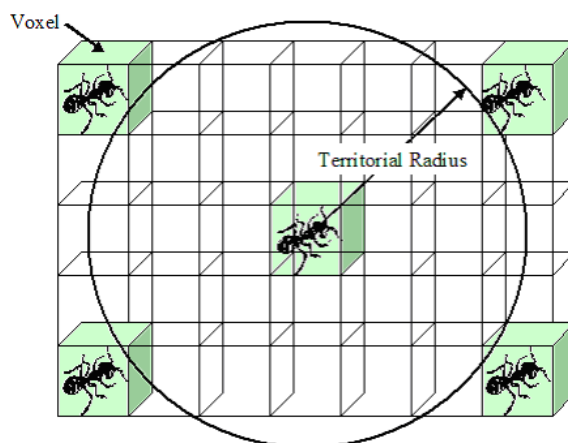


Figure-4: 2D Schematic illustrating the behavior of ant track attribute to search for the discontinuities inside the 3D cube.

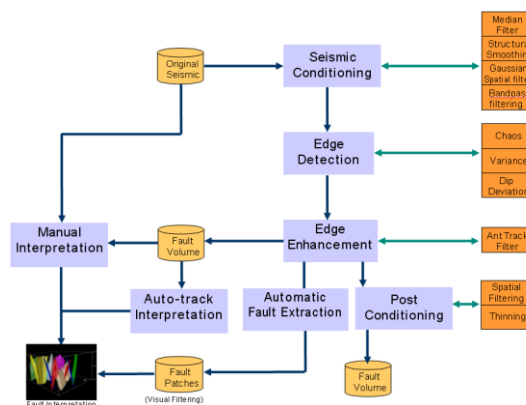


Figure-5: Schematic workflow showing the steps that have done before ant tracking attribute.

V. Ant Tracking Workflow

The patent pending Ant Tracking algorithm automatically extracts fault surfaces from fault attributes. The algorithm uses the principles from ant colony systems to extract surfaces appearing like trends in very noisy data. Intelligent software agents ("ants") will try to extract features in the attribute corresponding to expectations about the faults. True fault information in the attribute should fulfill these expectations and be extracted by many ants, whereas noise and remains of reflectors should be extracted by no ants or by only single ants (in which case they will be deleted). The approach is fully 3D and is able to take advantage of surface information in the surrounding voxels. This makes it possible to derive detailed information from the attribute. By writing the extracted surfaces back to a volume, we get what is referred to as an enhanced attribute, or ant track cube. This cube contains only what is likely to be true fault information.

The process can be divided into four main activities: (1) seismic conditioning, (2) edge detection, (3) edge enhancement, and (4) interactive interpretation (surface extraction). A collection of surface segments and fault patches can be extracted after the generation of the ant-track attribute. This is a volume of fault surface "pieces" having a high confidence of connectedness, which can be interactively merged into complete fault surfaces using the process. The main workflow can be seen in the illustration of Figure-6.

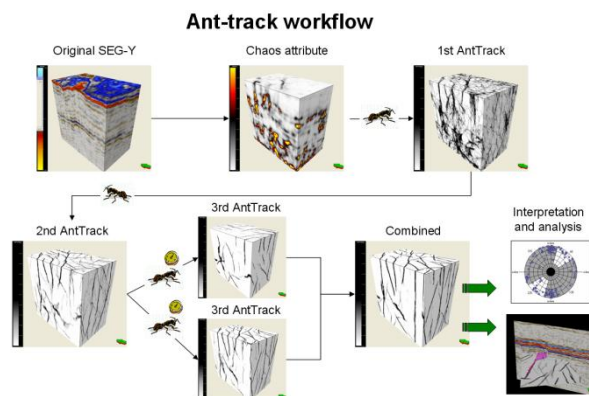


Figure-6: 3D Ant-track workflow illustrating the 3D approach for the attributed cube.

1. First, the original seismic data should be processed or conditioned using the structural smoothing option with the fault edge preservation option.
2. Then a Variance cube needs to be generated that will contain all the discontinuities.
3. Alternatively, the Chaos attribute can be generated instead.
4. Either the Variance cube or the Chaos cube can be used as input for the Ant Tracking process.
5. Any other input that enhances discontinuities can also be used (like Coherency for example). This volume needs to be loaded to Petrel first, either using the SEG-Y loader or the Open-Spirit connectivity.
6. Next, the Ant Tracking algorithm generates an enhanced Ant cube. This cube can be used for manual fault interpretation or, preferably, as input into the Automatic fault extraction process.

7. If the Automatic fault extraction process is used, based on the set parameters, extracted surfaces will be generated and saved under a separate folder.
8. The new workflow is a top-down approach, where the interpreter interacts with automatically extracted fault surfaces in a 3D canvas. Several properties are connected with the surfaces, which the interpreter can use for organizing the data. For example, the surfaces can be split into groups representing fault systems. The faults that make a system have common strike, meaning that the same stress field has created them in the same time period.

a) Structural smoothing attribute

To clear background of the seismic reflectivity and emphasize the amplitude, we should apply structural smoothing attribute that deals with smoothing of the input signal guided by the local structure (Figure-7) to increase the continuity of the seismic reflectors (Randen, 2002). Principal component dip and azimuth computation are used to determine the local structure. Gaussian smoothing is then applied parallel to the orientation of this structure. The filter size controls the number of traces horizontally and samples vertically to use for estimating structural smoothing. The value represents the standard deviation for the Gaussian filter. The larger the value, the larger number of traces and samples will be used. In terms of the number of traces or samples, it is approximately twice the value on either side of the current point (a standard deviation of 1.5 would use 3 traces on either side of the central point for a total of 7 traces in each direction).

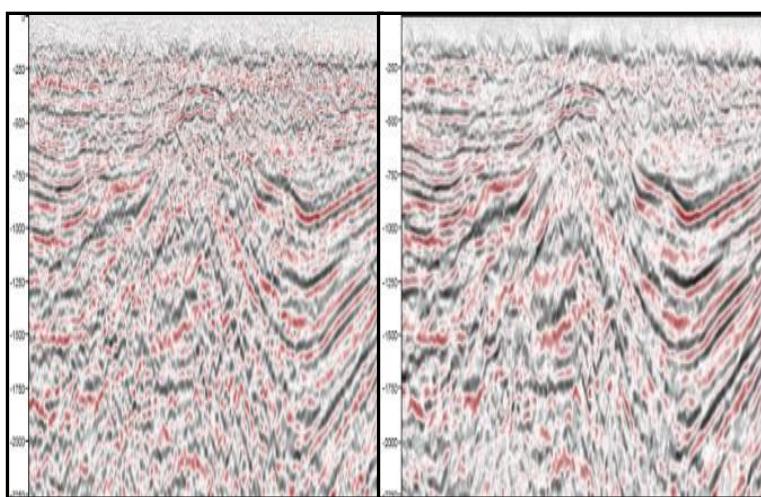


Figure-7: Segments of a seismic section (left) before and (right) after structural smoothing from a 3D volume from Ras El-Ush field, GOS, Egypt. Notice the cleaner background and focused amplitudes of the seismic reflections after smoothing as the preserved fault edges. (Data courtesy of Petrozeit)

The structural smoothing attribute can also be used to illuminate “flat spots” within the seismic volume. By running the smoothing operation without dip guiding, horizontal features such as fluid contacts can be emphasized. Structural smoothing is an extremely valuable operation to run before auto-tracking as it can stabilize the results. The results could be snapped back to the original data, or used as a smooth interpretation of regional surfaces. Structural smoothing helped in illustrating the reflectivity in the study area.

b) Chaos attribute

The chaotic signal pattern contained within seismic data is a measure of the “lack of organization” in the dip and azimuth estimation method. Chaos in the signal can be affected by gas migration paths, salt body intrusions, and for seismic classification of chaotic texture.

Chaos in the signal can be used to illuminate faults and discontinuities and for seismic classification of chaotic texture. Chaos can be related to local geologic features, as gas migration paths will affect it, salt body intrusions, reef textures, channel infill, etc.

Chaos is an edge detecting attribute (Figure-8) that helped in this study to improve the thickness of salt body and for the enhancement as well of the fault plane of the major clysmic fault in Ras El-Ush Field.

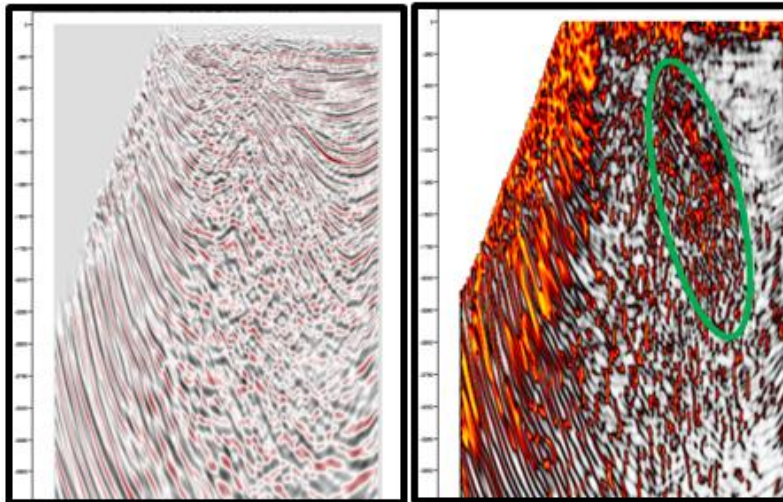


Figure-8: Segments of a seismic section (left) before and (right) after chaos attribute from a 3D volume from Ras El-Ush field, GOS, Egypt. Notice the Edge detecting of fault zone (Green oval) of the seismic reflections after application of smoothing and chaos (Variance) attributes as the preserved fault edges. (Data courtesy of Petrozeit)

This powerful tool is very useful in the study area (Figure-9) to filter correlated noise, for example, an acquisition footprint, and it helped in isolation of specific fault systems of Zig Zag fault Pattern at the rift borders and within the rift basins that resulted from reactivation and hard linkage of the NW-trending shear zones via N-S and NNE-SSW Fault. (Mcclay & Khalil-2009).

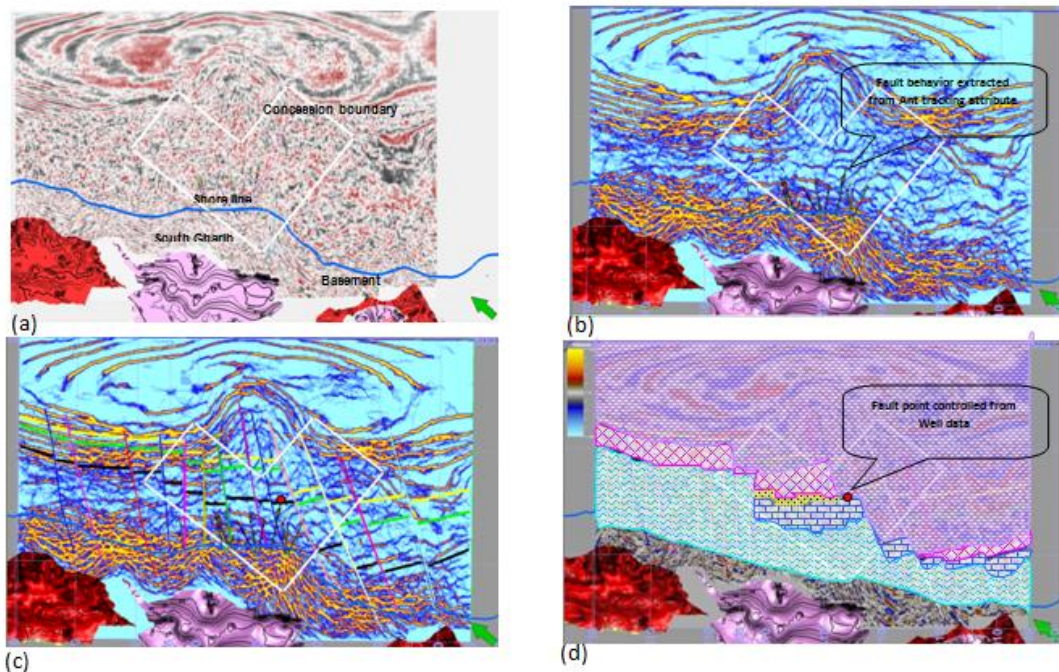


Figure-9: Depth slice at (-)691m penetrated by Ras El-Ush-6 well at Fault point of South Gharib Fm. (a) Original seismic depth slice (b) After applying ant tracking attribute (c) Fault interpretation of the attributed depth slice (d) Full interpretation of the depth slice controlled with well data and ant tracking attribute. Notice Fault point (Red circle) matched with the result of ant tracking attribute.

VI. Conclusion

The application of Ant tracking attributes that derived from the 3D seismic data at Ras El-Ush oil field show subsurface structural aspects of a buried volume of rock that would typically be beneath the resolution of traditional seismic amplitude data. The exact location of a seismic fault, that conformed with well data, and also the South West direction of the Ras El-Ush formations, that confirmed from well data but not confirmed by original seismic data, were also revealed. Comparison between 3D PSDM original data and attributed 3D seismic volume indicate that the applying 3D seismic attributes in the study area has been successful in delivering improved illumination. Faults are more clearly imaged and better continuity is observed at several levels. Implementation of 3D seismic Ant tracking attribute complemented offshore structural features such as downthrown trapping, subsalt structures, reservoir characterization examples such as fault interpretation and its relation to the existence of Hydrocarbon. Well ties with the result of derived seismic attributes increased the confidence as per the results obtained Figure-9. The first results of the seismic interpretation indicate significantly improved lateral and vertical resolution and provided higher confidence in mapping of faults and sedimentary features.

Acknowledgments

The authors thank Petrozeit Corporation for supplying the available data that used to conduct the present study and EGPC data center for their Permission to publish this paper.

References

- [1]. Barnes, Mary Cole, Terry Michaels, Phil Norlund and Chuck Sembroski (EAGE 2011) Making seismic data come alive.
- [2]. Kurt J. Marfurt (TLE, 2008) Emerging and future trends in seismic attributes.
- [3]. Aktepe and Marfurt (SEG 2007 Expanded Abstracts) Imaging of basement control of shallow deformation; application to Forth Worth Basin.
- [4]. Al-Bannagi et al. (TLE, 2005) Acquisition footprint suppression via the truncated SVD technique: Case studies from Saudi Arabia.
- [5]. Al Bin Hassan and Marfurt (SEG 2003 Expanded Abstracts) Fault detection using Hough transforms.
- [6]. Al-Dossary and Marfurt (GEOPHYSICS, 2006) Multispectral estimates of reflector curvature and rotation.
- [7]. Bergbauer et al. (AAPG Bulletin, 2003) Improving curvature analyses of deformed horizons using scale-dependent filtering techniques.
- [8]. Blumentritt (AAPG 2006 Annual Meeting) Volume-based curvature analysis illuminates fracture orientations.
- [9]. Carlson and Peloso (SEG 2007 Expanded Abstracts) Multi-attribute visual classification of continuous and fragmented seismic data.
- [10]. Castagna and Sun (First Break, 2006) Comparison of spectral decomposition methods.
- [11]. Chopra and Marfurt (TLE, 2007) Curvature attribute applications to 3D seismic data.
- [12]. Chopra and Marfurt (SEG CE Course, 2007) Seismic attributes for prospect identification and reservoir characterization.